Analytical Methods

Accepted Manuscript

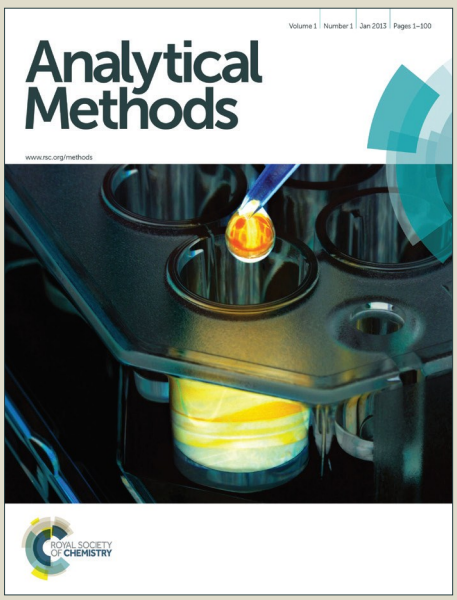

This is an *Accepted Manuscript*, which has been through the Royal Society of Chemistry peer review process and has been accepted for publication.

Accepted Manuscripts are published online shortly after acceptance, before technical editing, formatting and proof reading. Using this free service, authors can make their results available to the community, in citable form, before we publish the edited article. We will replace this *Accepted Manuscript* with the edited and formatted *Advance Article* as soon as it is available.

You can find more information about *Accepted Manuscripts* in the Information for Authors.

Please note that technical editing may introduce minor changes to the text and/or graphics, which may alter content. The journal's standard Terms & Conditions and the Ethical guidelines still apply. In no event shall the Royal Society of Chemistry be held responsible for any errors or omissions in this *Accepted Manuscript* or any consequences arising from the use of any information it contains.

ROYAL SOCIETY OF CHEMISTRY

www.rsc.org/methods

Journal Name

ARTICLE

An electrochemical impedance sensor for simple and specific recognition of G-G mismatches in DNA

Received 00th January 20xx,
Accepted 00th January 20xx

DOI: 10.1039/x0xx00000x

www.rsc.org/

Min Huang,[a] Hanying Li,[b] Hanping He,*[ab] Xiuhua Zhang[ab] and Shengfu Wang[a]

The sequence-specific recognition of SNPs is important for disease diagnosis and human gene therapy. In this work, a simple sensor based on electrochemical impedance spectroscopy (EIS) was developed for the highly sensitive and specific detection of G-G mismatches in dsDNA using a small molecule-modified gold electrode. After the electrochemical impedance sensor was incubated with G-G mismatched dsDNA, its charge-transfer resistance (R_{ct}) increased significantly. Meanwhile only a small increase in R_{ct} values was observed for dsDNA with other base mismatches and for complementary dsDNA. Importantly, G-G mismatched dsDNA was selectively detected based on differences in charge transfer resistance (ΔR_{ct}) even in the presence of other DNA and ct-DNA. Under optimal experimental conditions, the established EIS sensor was used to quantify G-G mismatched dsDNA based on the linear relationship between ΔR_{ct} and the logarithm of the concentration of G-G mismatched dsDNA from 1 nM to 1 μM with a detection limit of 0.3 nmol/L. This sensing strategy is a potential alternative tool for measuring G-G mismatched DNA for the diagnosis and early clinical detection of genetic diseases.

1.Introduction

In the last decade, much research has focused on the detection of specific nucleic acid sequences, particularly in the areas of medicine, biology and chemical biology. DNA detection plays an important role in the diagnosis of genetic diseases and is useful for early-stage monitoring and treatment.[1] Single nucleotide polymorphism (SNP) is a genetic difference bases on a single nucleotide base and is the most frequently observed variations in DNA sequence in the human genome. SNPs are present in every 500-1000 base pairs.[2-3] For example, DNA mutations include transitions, transversion, and the deletions etc. Many diseases are directly related to SNP, including cell anemia and cystic fibrosis, *etc*. Therefore, it is necessary to detect a difference in single nucleotides in DNA sequences, preferably using a technique that is reliable and affordable. [4-7]

Biosensor technologies have been investigated because of their great promise for the rapid, high sensitivity, and low-cost detection of specific DNA sequences related to human cancer, viruses, and bacterial.[8-10] Strategies for SNP detection based on biosensors have been based mainly on nucleic acids (e.g., peptide nucleic acids, and locked nucleic acids), surface ligation reaction (e.g., ligase-mediated gene detection), single base extensions, mismatch binding proteins, rolling circle amplification, and strand–displacement amplification and so on. The methods have theirselves advantage of better selectivity and sensitivity, especially rolling circle amplification that can arrive a detection limit about some amol/L concentration.[11] However, the process is of complex with high cost, needing operation of professional technician.

Electrochemical biosensors for detecting DNA have attracted much attention because of their high sensitivities, low-costs, simple

[a] Hubei Collaborative Innovation Center for Advanced Organic Chemical Materials; Ministry of Education Key Laboratory for the Synthesis and Application of Organic Functional Molecules, Hubei University, Youyi Road 368, Wuchang, Wuhan, Hubei 430062, (PR China).
[b] College of Chemistry and Chemical Engineering, Hubei University, Youyi Road 368, Wuchang, Wuhan, Hubei 430062, (PR China)
Corresponding author. Tel: +86-027-50865319; fax: +86-027-88663043.
E-mail addresses: hehanping@hubu.edu.cn
Electronic Supplementary Information (ESI) available: See DOI: 10.1039/x0xx00000x

operation and rapid responses.[12-16] Recently, electrochemical measurement protocols, e.g., chronocoulometry,[17] square-wave voltammetry,[18] differential pulse voltammetry,[19] and electrochemical impedance spectroscopy (EIS)[20-23] have been reported for the detection of DNA. Many of these sensors to detection SNPs were also based on DNA, PNA, locked nucleic acids, surface ligation reaction, single base extensions, mismatch binding proteins, rolling circle amplification, and strand–displacement amplification. Unfortunately, they also suffer from shortcomings in their stability and simplicity.

In previous work, some naphthyridine derivatives displayed excellent recognition for SNPs such as G-G mismatches.[24-30] Naphthyridine group was shown to form complementary hydrogen bonds with guanine base. Bi-functional probes containing both an electrochemically active group (ferrocenyl) and a DNA binding organic molecule through the condensation of carboxyl and amine have been developed for the electrochemical detection of DNA (including G-G mismatches and CGG repeats DNA) based on current changes.[31-33] Electrochemical impedance spectroscopy (EIS), which provides insight into interfacial reactions and mass transport processes in electrochemical systems,[34] has been widely used as a DNA label-free detection method to study various molecular binding processes, including antigen-antibody recognition, protein-DNA interactions, and DNA hybridization.[35-43] We recently developed an electrochemical impedance sensor for the detection of CGG trinucleotide repeats using EIS.[33] The electrochemical impedance sensor exhibited the very simple and rapid detection of CGG trinucleotide repeats with a label-free target DNA and without immobilizations of DNA. It is a very promising option for the early diagnosis and treatment of Fragile X syndrome.

In this work, because of low-cost and simple of the EIS, the approach would be developed for the detection of G-G mismatches in DNA duplexes. To the best of our knowledge, this is the first report of the specific detect of G-G mismatch duplexes by EIS based on small molecule modified electrode. The EIS exhibited a wide linear range, excellent detection limit with 0.3 nmol/L, and very good sensitivity. Importantly, the method is very simple, easy to operate, low-cost and label-free target. In addition a very good selectivity and stability was achieved even in the presence of other DNA and ct-DNA based on changes in the charge transfer resistance at the interface.

2Experimental Section

2.1 Reagents and Apparatus.

N-(3-dimethylaminopropyl)-N'-ethylcarbodiimide-hydrochloride (EDCI) was purchased from Sigma-Aldrich. N-hydroxysuccinimide (NHS), 2-(N-morpholino)-ethanesulfonic acid (MES), 3-mercapto propionic acid (MPA, 99%), were purchased from Aladdin Reagent Database Inc. (Shanghai, China). Phosphate buffer solution (PBS,10mM, pH=7.4), Tris-HCl (pH=7.4),ultrapure water (18.25 MΩ cm) was used in all experiments. All other reagents were analytical grade and used without further purification. Oligonucleotides were synthesized and purified by Sangon (Shanghai, China). All dsDNA was paired through the hybridization of ssDNA.

Electrochemical experiments, including electrochemical impedance spectroscopy (EIS) and square wave voltammetry (SWV) and cyclic voltammetry (CV) were conducted on a CHI 660C electrochemical workstation (CH Instruments, Inc. Shanghai) with a three-electrode system consisting of a Au electrode as working electrode, a saturated calomel electrode (SCE) as reference electrode, and platinum wire as counter electrode, respectively.

2.2. Preparation of the Sensor-Successive Steps of Gold Electrode Modification

The synthesis of the Boc-NC-linker has been reported previously.[33] Fig.S1 shows ^{1}H NMR and HRMS of of the synthesized molecules. Boc-NC-linker (8 mg, 1 mmol) was dissolved in 5 mL $CHCl_3$, and 4 mol/L HCl/EtoAc was added dropwise in an ice bath. The Boc-NC-linker reacted completely as determined TLC monitoring. The solvent $CHCl_3$ was removed, and remaining brown solid was washed in 1 mL $CHCl_3$ to remove undeprotected Boc-NC-linker. Finally, the solid was dried before being dissolved in 1 mL CH_3OH to obtain the 10 mM storage solution used in the next step.

A bare Au electrode (2 mm in diameter) was polished carefully with 0.05 μM alumina slurries for at least 10 min, before being ultrasonically cleaned with ethanol and ultrapure water twice for 5 min. The electrode was cleaned electrochemically in 0.5 mol/L H_2SO_4 by cycling the potential between -0.2 V and 1.6 V until a standard CV curve was obtained. Subsequently, the gold electrode was rinsed with ultrapure water and absolute ethanol. This as-pretreated bare gold electrode was immersed in an absolute ethanol solution containing 5 mM MPA, and was incubated at room

temperature for 12 h. The electrode was then removed and washed gently with ultrapure water to remove any excess MPA. The electrode was then immersed into the activation solution containing 400 mM EDCI and 100 mM NHS for 2 h. The activated gold electrode was then immersed in PBS containing 200 µM terminal amino group NC-linker for 3 h to form peptide bonds. The NC-linker modified electrode (EIS sensor) was obtained after washing with ethanol and ultrapure water to remove any weakly adsorbed material.

2.3 Electrochemical measurements

The modified gold electrode was immersed in different 20 mM solution containing mismatched dsDNA in Tris-HCl (pH=7.4) and incubated for different time at 37°C. Some electrochemical measurements were performed after washing to remove nonspecifically bound DNA. To characterize electrochemical changes at the electrode/electrolyte interface caused by the step by step deposition of MPA, NC-linker and G-G mismatched DNA. CV and EIS were performed for the prepared biosensor in the presence of the redox couple probe $[Fe(CN)_6]^{3-/4-}$. All electrochemical measurements were performed in an electrochemical cell at room temperature. For CV measurements, tests were performed using 4 mL solution containing 0.5 mM $K_3[Fe(CN)_6]$ and 0.5 mM $K_4[Fe(CN)_6]$ in 0.5 M aqueous potassium nitrate (KNO_3) over the potential range from -0.2 V to 0.6 V at a scan rate of 0.1 V/S. SWV were performed in the same solution as was used for CV measurement. SWV experiments were performed from -0.1 V to 0.65 V with an increment 0.004 V, and an amplitude of 0.025 V at a frequency 15Hz and quiet time of 2s. The impedance measurements were performed in the same solution by applying an AC voltage with an amplitude of 5mV in a frequency range from 0.01 Hz to 100 kHz at under 0.208 V. The electrical circuit parameters were determined by fitting the impedance data to the equivalent circuit shown in Fig. 1. The fits were performed over the total frequency range from 0.01 Hz to 100 kHz using a non-linear least-squares fit, which was performed using ZSimpWin software (Princeton Applied Research Massachusetts, USA).The ZSimpWin software pakage was used to fit the Nyquist plot, which contained the real (Z′) and imaginary components (-Z″) of the immobilized layers' resistances, and the equivalent circuit was used to understand the surface structure. From the values of R_{ct}, the quantitative signal was determined as a function of DNA concentration using the increasing R_{ct} after the NCD/MPA/Au sensor was incubated with different DNA concentrations of DNA.

3. Results and Discussion

3.1 Sensing principle

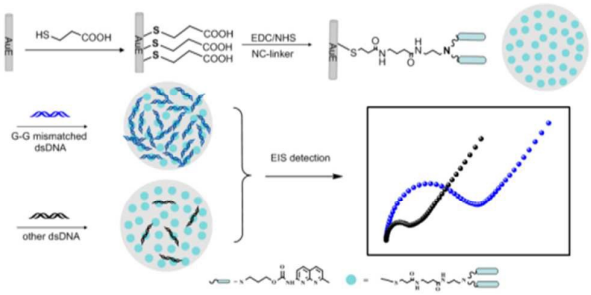

Scheme 1. Schematic diagram of the proposed EIS-based biosensor for DNA detection

The principle of EIS detection (Scheme 1) for the sequence-specific recognition of G-G mismatched DNA was effective, rapid and affordable, making it useful for practical applications. Based on previous work, naphthyridine derivatives were successfully applied as recognition molecules in electrochemical impedance method. Briefly, NCD was immobilized on the surface of an Au electrode using a flexible long chain to create an EIS biosensor. The recognition of G-G mismatched dsDNA was achieved by monitoring differences in R_{ct} before and after incubation of the EIS biosensor in target DNA solution. MPA were first self-assembled on the surface of the Au electrode to couple NC-linker compound via amide linkage. NC-linker modified Au electrodes (EIS biosensor) were used to bind with target duplexes via hydrogen bonding. When the duplexes were selectively bound to NC molecule, the DNA on the surface of the Au electrode blocked interfacial charge transfer, which resulted in increasing charge-transfer resistance (R_{ct}). The different DNAs were distinguished by the difference changes in R_{ct} value. In the target dsDNA, G-G mismatched DNA was specifically bound to NC (as has been shown in our previous work). Therefore the EIS sensor had a higher R_{ct} after being incubated with G-G mismatched dsDNA, allowing it to be differentiated from other mismatched DNAs.

3.2 Characterization of the Modified Electrode

Electrochemical behaviors of the modified electrodes were characterized at different stages using EIS, SWV, and CV experiments. As shown in Fig.1, EIS curves, obtaining in 0.5 M KNO_3 containing 0.5 mM $Fe(CN)_6^{3-/4-}$, contained the semicircles diameter of which were equal to R_{ct}. The curve of EIS presented as Nyquist plots,

consisting of two portions: (1) the semicircle section at high frequencies, which corresponds to R_{ct} and (2) a linear portion at low frequencies, which is related to diffusion-limited processes in solution.[44] The equivalent circuit was used to fit the impedance data as shown in the inset to Fig.1. In the equivalent circuit, R_1 and W_1 are the resistance of the solution and the Warburg impedance, respectively. R_{ct}, which was caused by charge transfer reactions (Faraday processes) and the diffusion of ions from the electrolyte to the interface, and the interfacial double layer capacitance were treated as constant phase elements. The fit in Fig.1 shows that the experiment curves are in a good agreement with the fits. In a 0.5 M KNO_3 solution containing 0.5 mM $Fe(CN)_6^{3-/4-}$, the bare electrode exhibited an almost straight line (curve a) reflecting the outstanding electrochemical conductivity of the bare Au. After the self-assembly of MPA on the bare electrode via-thiol binding, the value of R_{ct} increased (curve b) to 2899 ohm from 221 ohm (ΔR_{ct}/ohm =2678). This was attributed to the small molecules obstructing electron transfer. Afterwards, NC-linker compound was coupled to the carboxyl on the electrode's surface via condensation reaction. R_{ct} slightly increased (curve c). R_{ct} of the fitting curves changed to 6087 ohm from 2899 ohm (ΔR_{ct}/ohm =3188). This increased impedance indicated that the interface of the EIS sensor was prepared successfully.

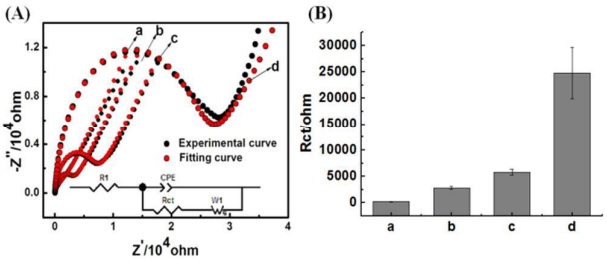

Fig.1 (A) The Nyquist plots of different modified electrodes in the frequency range from 0.01 Hz to 100kHz: (a) bare/Au electrode, (b) MPA/Au electrode, (c) NCD/MPA/Au electrode (EIS sensor), and (d) EIS sensor after incubation with G-G mismatch DNA. The inset displays the equivalent circuit used to fit the experimental EIS data. (B) Histograms representing average R_{ct} values obtained. RSDs ranged from 0.4 to 5.7%.

After the EIS sensor was further incubated with target G-G mismatched duplex (0.5 µmol/L), R_{ct} increased significantly (curve d). The value of R_{ct} jumped from 6087 ohm to 24820 ohm (ΔR_{ct}/ohm =18733), indicating that the EIS sensor effectively captured G-G mismatched DNA by hydrogen bond interactions. More negative charges were introduced onto the electrode's surface, causing diffusion of redox probe to the surface of the electrodes to be hindered by repulsive interactions.[45] These results were in a good agreement with those obtained from SWV measurements (Fig.2A) and CV measurements (Fig.2B), in which the peak currents changed during the assembly and binding processes. These results further indicated the successful assembly and binding of DNA, as described in scheme 1 and eliminated the possibility of false positive in the impedimetric assay.

The appearent fractional coverage (θ^R_{IS}) of each modification of gold electrode were calculated according the Eq. (1) described by Janek et al[46]

$$\theta^R_{IS} = 1 - \frac{R_{ct}^{bare}}{R_{ct}^{m}} \quad (1)$$

Where bare and m represented the bare Au electrode and each modified electrode respectively. The calculated θ^R_{IS} values were give in Table S1. The values of θ^R_{IS} were increasing, and more than 0.9, which indicated successful modification and most full coverage at gold surface.

$$\theta^R_{IS} = 1 - \frac{R_{ct}^{before}}{R_{ct}^{after}} \quad (2)$$

In addition, the appearent fractional coverage (θ^R_{IS}) of dsDNA captured on NCD/MPA/Au electrode was calculated by the Eq. (2) similarly.[46,47] Where, before and after represented NCD/MPA/Au electrode before and after incubation with dsDNA respectively. θ^R_{IS} based on R_{ct} values before and after incubation with dsDNA on NCD/MPA/Au electrode was 0.766 when the concentration of dsDNA was 0.5 µmol/L. The values of θ^R_{IS} at other concentrations can be seen in following (Table S2).

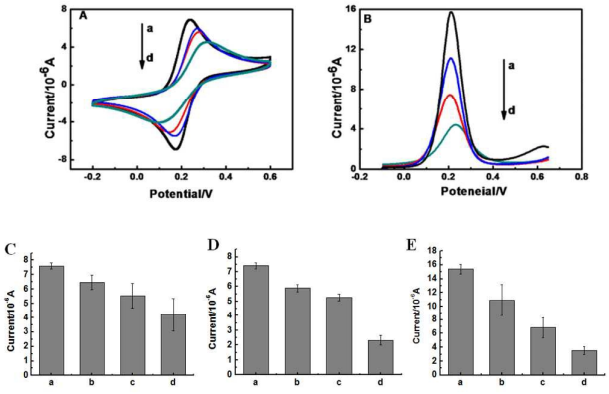

Fig.2 CV (A) and SWV (B) response of the(a) bare/Au electrode, (b) MPA/Au electrode, (c) EIS sensor, and (d) EIS sensor after incubation with G-G mismatched DNA. Histograms representing average anodic (I_{pa}) (C) and cathodic (I_{pc}) (D) values of CV obtained. (E) Histograms representing average current from the obtained SWV. RSDs ranged from 0.6 % to 5.4 %.

3.3 Optimization of incubation time

The capture of DNA by NC-modified electrode requires sufficiently long incubation time because of the dynamic equilibria and thermodynamics of the interaction between the NC and DNA. As shown in Fig.S3, the impedance of the EIS sensor after incubation with target DNA increased with incubation time before reaching nearly constant value after 80 min, suggesting means that the binding on the surface of the electrode reached saturation. For this reason, 80 min was used as the incubation time for target DNA in the electrochemical tests described in the following section.

3.4 Selectivity

To further investigated the sensor's effective sequence-specific recognition of G-G mismatch DNA, 16 kinds of dsDNA including G-G mismatched, other mismatched duplexes (G-A, G-T, C-A, C-T, C-C, A-G, A-A, A-C, T-G, T-T, and T-C) and complement DNA(G-C, C-G, A-T, T-A) were used in the assay. The detailed DNA sequences are provided in the supporting information. The ESI spectra and R_{ct} values of the electrodes were recorded before and after incubation with these dsDNA targets. As shown in Fig.3, black points show R_{ct} after incubation with the G-G mismatched duplex. Clearly, these black points had the larger R_{ct} value (2.5×10^4 ohm) than did the other duplexes shown in Fig.3. This corresponded to ΔR_{ct} value as larger ad 18906 ohm in the presence of G-G mismatched DNA, which was 2.65 to 39 times higher than the values of other duplexes (Fig.4). These data strongly indicated that the EIS sensor successfully captured more G-G duplexes than other duplexes and had an excellent selectivity for G-G mismatched dsDNA. For other DNA, the values of ΔR_{ct} were generally between 480 ohm and 7120 ohm, because of nonspecific interactions between the small molecule and DNA.

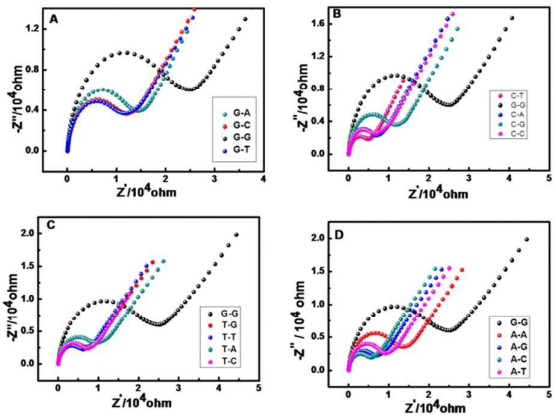

Fig.3 EIS of the different electrodes:(A)EIS sensor after incubation with 0.5 μmol/L G-X(X=G, T, C, or A) DNA (B) EIS sensor after incubation with 0.5 μmol/L G-G/C-X (X=G, T, C, or A) DNA (C) EIS sensor after incubation with 0.5 μmol/LG-G/T-X(X=G, T,C, or A) DNA (D) EIS sensor after incubation with 0.5 μmol/LG-G/A-X(X=G, T, C, or A) DNA.

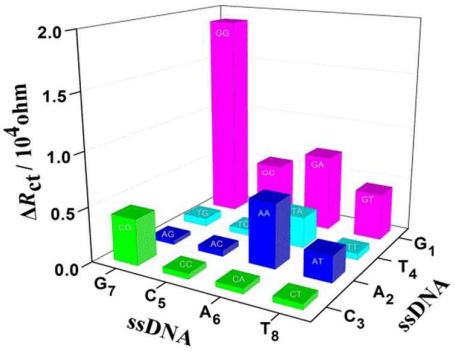

Fig.4 ΔR_{ct} of the EIS sensor after incubation with the 16 kinds of dsDNA.

3.5 Detection of Target DNA

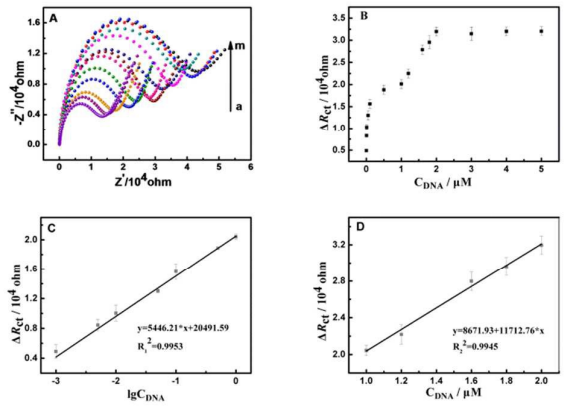

Fig.5 EIS response of the EIS sensor after incubation with different concentrations of G-G mismatched DNA at concentrations of 1, 5, 10, 50, 100, 500,1000,1200, 1600, 1800, 2000, 3000, 5000 nmol/L, corresponding to a to m, respectively (A). The relationships between ΔR_{ct} and target DNA concentration (B). The first linear region of ΔR_{ct} *vs.* the logarithm of the target concentration from 1 nM to 1 μM(C). The second linear region of ΔR_{ct} *vs.* the target concentration from 1 μM to 2 μM (D).The relative standard deviations (RSDs) of three parallel experiments were between 0.4% and3.5%.

Under optimal conditions, different concentrations of target G-G mismatched DNA were analyzed with EIS measurements in 0.5 M KNO_3 containing 0.5 mM $Fe(CN)_6^{3-/4-}$ using the EIS sensor. As shown in Fig.5, it was found that R_{ct} increased with increasing concentration of dsDNA until reaching saturation. Initially, the values of R_{ct} were particularly sensitive to concentrations before a small plateau was reached. Above 1 μmol/L, the sensitivity increased again before finally reaching saturation, as shown in Fig.5B. Two linear regions were observed as shown in Fig.5C and Fig.5D. The plot of ΔR_{ct} *vs.*the logarithmic of the target DNA concentration was linear from 1 nmol/L to 1μmol/L with a detection limit of 0.3 nmol/L. The linear fit followed ΔR_{ct} = 5446.21×lgC_{DNA}+20491.59 and had a correlation coefficient of R_1^2 = 0.9953. In the other linear range, ΔR_{ct} *vs.* the target DNA concentration was linear from 1 μmol/L to 2 μmol/L, with a linear fit of ΔR_{ct} = 8671.93×C_{DNA}+11712.76 with a correlation coefficient of R_2^2=0.9945. In the preparation of modified electrode, the appearent fractional coverage (θ^R_{IS}) was discussed. Here, θ^R_{IS} before and after incubation with different concentrations of the dsDNA on NCD/MPA/Au electrode was calculated according the Eq. (2) for ability to capturing target DNA. The details can be seen in table S2. θ^R_{IS} values were increasing until a plateau when the concentrations of dsDNA increased from 0.01 μmol/L to 5 mol/L. The higher θ^R_{IS} values indicated excellent capturing ability of EIS sensor.

3.6 Interference, stability, and repeatability of the sensor

According to the results presented above, the assay was very simple and rapid while providing an excellent selectivity and sensitivity. To conveniently use this method for practical samples, tests were performed on mixtures that contained different potentially interfering DNA including ct-DNA. EIS sensors were incubated with mixture containing G-G mismatched DNA and five-times more of another DNA with a different base-pair DNA, as shown in Fig.6A. R_{ct} did not increased as much as it did in the presence of the G-G mismatched duplex alone, indicating that other mismatched DNA and complementary DNA did not interfere with the detection of G-G mismatched duplexes. Meanwhile, 16different duplexes mixtures were investigated, as shown in Fig.6B. The mixtures' ΔR_{ct} values clearly increased in the presence of G-G mismatched duplex. ΔR_{ct} was about three times larger in G-G mismatch duplex than in the mixture without G-G mismatch duplexes, even when the total concentration of the other 15DNA was about three times higher than that of the G-G mismatched duplexes. A fully matched double strand calf thymus DNA (ct-DNA) was also test (Fig.6B). When the concentration of ct-DNA was increased to as high as 2.5 μg/mL, ΔR_{ct} remained very small at only, 708 ohm. Fortunately, ΔR_{ct} increased to 20186 ohm when the ct-DNA sample contained 0.5 μM of the target G-G mismatched dsDNA. These results provided additional evidence that the EIS biosensor was able to detect a target with high specificity and had great potential for the recognition and detection of G-G mismatched dsDNA.

During these experiments, the EIS sensor was high stable and repeatable. In the experiment reported above (including the optimization of incubation time, and the determination of selectivity and linearity relationships), the relative standard deviations (RSDs) of three parallel measurements ranged from 0.4% to 6.4%. Finally, four different electrodes were treated using the same procedure to test the reproducibility of the method. The RSDs was 6.6% for the determination of 500 nM target DNA under the same conditions (Fig.S4). These results indicated that the assay was

reliable and reproducible, important characteristics for practical applications.

For this assay, the EIS sensor was highly selective for G-G mismatched duplexes even when the target concentration was outside of the sensor's linear arrange. When 5 μM target duplex was measured in the assay, the ΔR_{ct} for the G-G mismatched duplex (3.5×10^4 ohm) was significantly larger than that measured for the other duplexes (between 230 ohm and 8900 ohm) (Fig.S5).

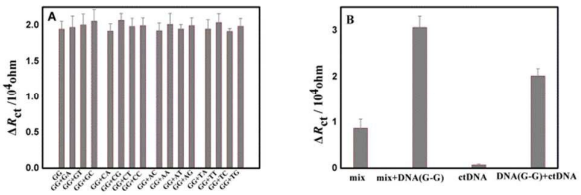

Fig.6 Selectivity of the EIS sensor after incubation with different mixtures. (A) 0.5 μmol/L target G-G mismatched DNA +2.5 μmol/L 15 other dsDNA sample respectively. (B) 1.65 μmol/L mixture of all 15 other DNA with and without 0.5 μmol/L target G-G mismatched DNA; 2.5 μg/mL ct-DNA with and without 0.5 μmol/L target G-G mismatched DNA. RSDs of three times experiments ranged from 0.8% to 4.3%.

4. Conclusion

A simple, sensitive, and flexible electrochemical method for the detection of G-G mismatched dsDNA was developed by EIS based on small molecule modified electrode. Recognition and detection were achieved by measuring R_{ct} values before and after incubation with target DNA. The method was so different from other DNA sensors utilizing olignucleotides as probe fragments and working either in hybridization modes including PNA and LNA. EIS method by PNA or LNA was not found for the detection of SNPs, as we known. Some other methods were reported for detection of SNPs by PNA and LNA, such as electrochemical method and fluorescence, as listed in table S3.

The EIS assay provided a very different idea for detection platform of SNPs. Although the detection limit didn't achieve very low concentration, the EIS sensor displayed a wide linear detection range (1 nmol/L to 1μmol/L) and excellent detection limit with a 0.3 nmol/L. The sensor have some advantages such as excellent specificity and reproducibility, simple preparation, rapid detection, low-cost, label-free target DNA, and no need professional technician when used. Moreover, the sensor was not affected by interferences by other duplexes and was able to discriminate target G-G mismatched DNA from 16 other DNA samples and a large, fully matched ct-DNA. Therefore, this EIS sensor is very useful platform for the SNPs detection especially for detection of G-G mismatched DNA.

Acknowledgements

H. P. He gratefully acknowledges support from the National Natural Science Foundation of China (Grant 21575035), and Foreign Science and Technology Cooperation Fund of Hubei province, China (2015BHE025).

Notes and references

1 X. Q. Zhu, J. Li, H. P He, M. Huang, X. H. Zhang and S. F. Wang, *Biosens. Bioelectron.,* 2015, **74,** 113-133.

2 E. S. Lander, L. M. Linton, B. Birren, C. Nusbaum, M. C. Zody, J. Baldwin and R. Funke, *Nature,* 2001, **409,**860-921.

3 J. C. Venter, M. D. Adams, E. W. Myers, P. W. Li, R. J. Mural, G. G. Sutton and J. D. Gocayne, *Science,* 2001, **291,**1304-1351.

4 J. Burmeister, V. Bazilyanska, K. Grothe, B. Koehler, I. Dorn, B. D. Warne and E. Diessel, *Anal. Bioanal. Chem.,*2004, **379,** 391-398.

5 A. J.Schafer and J. R. Hawkins, Nat. Biotechnol., 1998, 16, 33-39.

6 F. S.Collins, M. S.Guyer and A.Chakravarti,*Science,*1997, **278,** 1580-1581.

7 N. Risch and K. Merikangas, *Science,*1996, **273,**1516-1517.

8 N. Zainudin, A. R. M. Hairul, M. M. Yusoff, L. L. Tan and K. F. Chong, *Anal. Methods,*2014, **6,**7935-7941.

9F. F. Deng, C. Ding, Y. Wang, W. T. Li, L. L. Liu and H. Li, *Anal. Methods,* 2014, **6,** 9228-9233.

10 A. Chua, C. Y. Yean, M. Ravichandran, B. H. Lim and P. Lalitha, *Biosens. Bioelectron.,* 2011, **26,**825-3831.

11 S. B. Zhang, Z. S. Wu, G. L. Shen, R. Q. Yu, *Biosens.Bioelectron.,* 2009, **24,** 3201-3207.

12 H. Zheng, X. Ma, L. Chen, Z. Lin, L. Guo, B. Qiu and G. Chen,*Anal. Methods,* 2013, **5,** 5005-5009.

13 S. N. Topkaya, D. Ozkan-Ariksoysala, B. Kosova, R. Ozelb and M. Ozsoza, *Biosens. Bioelectron.,* 2012, **31,** 516-522.

14 Y. Qian, C. Y. Wang and F. L. Gao, *Biosens. Bioelectron.,* 2015, **63,**425-431.

15 J. Zhang, J. H. Chen, R. C. Chen, G. N. Chen and F. F. Fu, *Biosens. Bioelectron.,* 2009, **25,** 815-819.

16 J. H. Chen, J. Zhang, K. Wang, X. H. Lin, L. Y. Huang and G. N. Chen,

Anal. Chem., 2008, **80,** 8028-8034.

17 E. M. Boon, D. M. Ceres, T. G. Drummond, M. G. Hill and J. K. Barton, *Nat. Biotechnol.,* 2000, **18,** 1096-1100.

18 M. Inouye, R. Ikeda, M. Takase, T. Tsuri and J. Chiba, *Proc. Natl. Acad. Sci. U.S.A.,*2005, **102,** 11606-11610.

19 T. Ihara, M. Nakayama, M. Murata, K. Nakano and M. Maeda, *Chem. Commun.,* 1997, **17,**1609-1610.

20 E. Katz and I. Willner, *Electroanal,* 2003, **15,** 913-947.

21 F. Patolsky, A. Lichtenstein and I. Willner, *Nat. Biotechnol.,* 2001, **19,** 253-257.

22 Y. T. Long, C. Z. Li, T. C. Sutherland, H. B. Kraatz and J. S. Lee, *Anal. Chem.,* 2004, **76,** 4059-4065.

23 J. Y. Liu, S. J. Tian, P. E. Nielsen and W. Knoll,*Chem. Commun.,* 2005, **23,**2969-2971.

24 M. Nomura, S. Hagihara, Y. Goto, K. Nakatani and C. Kojima, *Nucleic Acids Symp Ser.,* 2005, **49,**213-214.

25 K. Nakatani, S. Sando and I. Saito, *Bioorg. Med. Chem.,* 2001, **9,** 2381-2385.

26 X. Li, H. Song, K. Nakatani and H. B. Kraatz,*Anal. Chem.,* 2007, **79,** 2552-2555.

27 K. Nakatani, S. Sando, H. Kumasawa, J. Kikuchi and I. Saito, *J. Am. Chem. SOC.,*2001, **123,**12650-12657.

28 K. Nakatani, A. Kobori, H. Kumasawa and I. Saito, *Bioorg. Med. Chem. Lett.,* 2004, **14,** 1105-1108.

29 K. Nakatani, A. Kobori, H. Kumasawa, Y. Goto and I. Saito, *Bioorg. Med. Chem.,* 2004, **12,** 3117-3123.

30 J. Li, H. P. He, X. Q. Peng, M. Huang, X. H. Zhang and S. F. Wang, *Analytical. Sciences,* 2015, **7,** 663-667.

31 H. P. He, J. P. Xia, G. Chang, X. Q. Peng, Z. W. Lou, K. Nakatani, X. Zhou and S. F. Wang, *Biosens. Bioelectron.,* 2013, **42,** 36-40.

32 H. P. He, J. P. Xia, X. Q. Peng, G. Chang, X. H. Zhang, Y. F. Wang, K. Nakatani, Z. W. Lou and S. F. Wang, *Biosens. Bioelectron.,* 2013, **49,**282-289.

33 H. P. He, X. Q. Peng, M. Huang, G. Chang, X. H. Zhang and S. F. Wang, *Analyst,*2014, **139,** 5482-5487.

34 M. Chen, C. Y. Du, G. P. Yin, P. F. Shi and T. S. Zhao, *Int. J. Hydrogen. Energ.,* 2009, **34,** 1522-1530.

35 C. Ocaña, M. Pacios and M. del Valle, *Sensors,* 2012, **12,** 3037-3048.

36 A. Hayat, A. Sassolas, J. L. Marty and A. E. l. Radi, *Talanta,*2013, **103,** 14-19.

37 D. T. Tran, V. Vermeeren, L. Grieten, S. Wenmackers, P. Wagner, J. Pollet and J. Lammertyn, *Biosens. Bioelectron.,* 2011, **26,** 2987-2993.

38 C. Ocaña, E. Arcay and M. del Valle, *Sensor. Actuat. B-Chem.,* 2014, **191,** 860-865.

39 E. Eksin, A. Erdem, A. P. Kuruc, H. Kayi and A. Öğünç, *Electroanalysis,* 2015, **27,** 2864-2871.

40 J. Y. Park and S. M. Park, *Sensors,* 2009, **9,** 9513-9532.

41 A. Li, F. Yang, Y. Ma and X. Yang, *Biosens. Bioelectron.,* 2007, **22,** 1716-1722.

42 W. S. Yang, J. E. Butler, J. N. Russell. Jr and R. J. Hamers, *Analyst,* 2007, **132,** 296-306.

43 X. Yu, R. Lv, Z. Ma, Z. Liu, Y. Hao, Q. Li and D. Xu, *Analyst,* 2006, **131,** 745-750.

44 X. Jing, X. Cao, L. Wang, T. Lan, Y. Li and G. Xie, *Biosens. Bioelectron.,*2014, **58,** 40-47.

45 Z. Yang, B. Kasprzyk-Hordern, S. Goggins, C. G. Frost and P. A. Estrela, *Analyst,*2015, **140,**2628-2633.

46 R. P. Janek, W. R. Fawcett, *Langmuir* 1998, **14**, 3011-3018.

47 A. Erdem, G. Congur, *Int J Biol Macromol* 2013, **61**, 295-30.

Graphics abstract